Ab initio Calculation of the ^{17}O and ^{1}H NMR Parameters for Various OH Groups: Implications to the Speciation and Dynamics of Dissolved Water in Silicate Glasses

Xianyu Xue* and Masami Kanzaki

Institute for Study of the Earth's Interior, Okayama University, Misasa, Tottori, 682-0193 Japan

Received: November 7, 2000; In Final Form: February 13, 2001

Ab initio molecular orbital calculations have been carried out for silicate, aluminosilicate, and aluminate clusters to study the NMR characteristics of various types of hydroxyls (OH) that are possibly present in hydrous silicate glasses and melts. The clusters have been optimized with the density functional theory (B3LYP/6-311+G(2df,p)) and their NMR parameters calculated at HF/6-311+G(2df,p). Our calculations suggest that the ^{17}O and ^{2}H quadrupolar coupling constants (C_Q^O and C_Q^H) and ^{1}H chemical shift (δ_i^H) of SiOH, AlOH, and bridging OH's (Si(OH)Al, Al(OH)Al) all show good correlation with the O−H and O−H···O distances. The calculated C_Q^O, C_Q^H, and δ_i^H values agree well with those of the experimental data for OH groups with similar O−H···O distances in crystalline phases. Hydroxyls with stronger hydrogen bonding tend to yield smaller C_Q^O and C_Q^H and larger δ_i^H. SiOH and bridging OH's of comparable hydrogen-bonding strengths give similar ^{17}O and ^{1}H (^{2}H) NMR parameters. AlOH have a tendency not to form strong Al−O−H···O type hydrogen bonding and, thus, give relatively large C_Q^O and C_Q^H and small δ_i^H. On the basis of these calculation results, together with information for hydrogen-bonding strengths estimated from experimental vibrational spectra and ^{1}H NMR data, we were able to predict ^{17}O NMR parameters for hydroxyls in hydrous silicate glasses. The observed ^{17}O NMR peaks for silica gel and hydrous albite glass, that have been attributed to SiOH, are significantly narrower than expected from C_Q^O, suggesting that at least some of the SiOH, if present, must be nonrigid. The observed broad ^{17}O NMR peaks for hydrous albite and alkali silicate glasses, originally attributed to molecular H_2O, could equally well be ascribed to rigid hydroxyls with weak hydrogen bonding.

Introduction

The dissolution of water in silicate melts significantly affects their phase relations and physical/thermodynamic properties. The mechanism of water dissolution has been investigated on quenched silicate glasses by various spectroscopic techniques, such as infrared (IR), Raman, neutron diffraction, and nuclear magnetic resonance spectroscopy (NMR) [see a recent review (ref 1)]. It is now well-established, mostly from IR studies, that water is dissolved in silicate melts/glasses mainly as hydroxyls (OH) at low water concentrations and as both molecular water and hydroxyls at higher concentrations.[2−4] For aluminum-free silicate compositions (silica and alkali silicates), ^{29}Si NMR studies have revealed the presence of silanols (SiOH) in the quenched hydrous glasses, suggesting that the dissolved water has ruptured the silicate tetrahedral network (Si−O−Si linkages).[5−8] For aluminosilicate compositions, there were also suggestions that similar depolymerization of the network structure, that leads to the formation of SiOH and AlOH groups, may occur upon water dissolution.[9−11] Kohn and co-workers,[12−14] on the other hand, proposed that the dissolution of water merely causes exchange of H^+ and metal cations (M, e.g., Na^+ for sodium aluminosilicates), leading to the formation of protonated bridging oxygens (also referred to as bridging OH's) and MOH complexes. Their argument was mainly based on ^{29}Si, ^{27}Al, and ^{23}Na NMR data; the uniqueness of the spectral interpretation has, however, been questioned.[15] In addition to speciation distribution, there are other issues of interest concerning water dissolution, including the hydrogen-bonding strength, the spatial relationship, and dynamics of the dissolved water species.

The ^{17}O and ^{1}H (^{2}H) NMR are potentially useful techniques that might shed light on all these issues, because they can give direct information about the dissolved water species. There have been a number of ^{1}H and ^{2}H NMR studies on hydrous silicate glasses and gels.[11−14,16−22] Experimental NMR data on crystalline phases[18,19] and theoretical calculations[23] have established that the ^{1}H chemical shift and ^{2}H quadrupolar coupling parameters of OH groups (both molecular H_2O and hydroxyls) are dominated by the strength of the O−H···O type hydrogen bonding. ^{1}H and ^{2}H NMR have also been used to distinguish between H_2O and hydroxyls.[14,17−20,22] Variable-temperature ^{1}H and ^{2}H NMR studies have revealed that, at least for the dissolved molecular H_2O in silicate glasses, motions (possibly flipping motion) are detectable at room temperature and even at low temperature for certain compositions.[14,16,18,21] The ^{17}O NMR has also been increasingly utilized in recent years to yield high-resolution spectra, thanks to the development of new NMR techniques for half-integer quadrupolar nuclei, such as the dynamic angle spinning (DAS), double rotation (DOR), and multiple quantum magic angle spinning (MQ-MAS) NMR methods. A ^{17}O NMR study of hydrous $Na_2Si_4O_9$ and albite ($NaAlSi_3O_8$) glasses[24] revealed more than one ^{17}O NMR peaks that are absent for the corresponding anhydrous glasses. A relatively narrow peak in the $^{1}H-^{17}O$ cross-polarization (CP) NMR spectra, collected with short contact times, for both compositions has been attributed to SiOH groups. An extra peak in the ^{17}O MQ-MAS NMR spectra of the same glasses was also interpreted in a similar way. There is also a broad peak in ^{17}O saturation MAS NMR spectra for both glasses, which has

* To whom correspondence should be addressed. Phone: 81-858-43-3824. Fax: 81-858-43-2184. E-mail: xianyu@dbmac1.misasa.okayama-u.ac.jp. E-mail: mkanzaki@misasa.okayama-u.ac.jp.

10.1021/jp0040751 CCC: $20.00
Published on Web 04/06/2001

been attributed to dissolved molecular H_2O. However, uncertainties remain concerning the spectral interpretation of ^{17}O NMR data for the following reasons: (1) There is a lack of knowledge about the ^{17}O NMR characteristics of SiOH, AlOH, and bridging OH's with various hydrogen-bonding strengths, because experimental ^{17}O NMR data on relevant crystalline compounds are scarce and (2) Our earlier ab initio molecular orbital calculation results have suggested that SiOH with weak to moderate hydrogen-bonding strengths should yield larger C_Q^O and thus broader ^{17}O MAS or static NMR peaks than that assigned to SiOH in the experimental NMR work.[24] A systematic experimental ^{17}O NMR study on model crystalline compounds is one way to learn the ^{17}O NMR characteristics of such species. One such study on a crystalline hydrous silicate ($KHSi_2O_5$) phase containing SiOH[25] has been published after the submission of this paper and more are expected in the future. A complementary method is to calculate accurately their NMR parameters theoretically.

The ab initio molecular orbital (MO) calculation method is becoming increasingly reliable in predicting geometry and NMR and other spectroscopic properties with the rapid increase in computer power. There have been a number of previous ab initio calculations that bear on the ^{29}Si and ^{27}Al NMR characteristics,[26,27] ^1H NMR characteristics,[28,29] and vibrational properties[30−32] of hydrous silicates and aluminosilicates and many more on silicates and aluminosilicates in general. One advantage of the theoretical approach is that one can systematically investigate the effect of a particular structural factor, such as the strength of hydrogen bonding, on the NMR parameters.

In this paper, we report ^{17}O, ^1H, and ^2H NMR parameters for SiOH, AlOH, and bridging OH (Si(OH)Al and Al(OH)Al) groups in silicate, aluminosilicate, and aluminate clusters, calculated using the ab initio MO method. This is part of an ongoing effort to study the ^{29}Si, ^{27}Al, ^{17}O, ^1H, and ^2H NMR characteristics of structural units that are potentially present in silicates, aluminosilicates, and aluminates (both hydrous and anhydrous). We have previously reported the ^{29}Si and ^{27}Al NMR results, as well as the ^{17}O NMR results for bridging oxygens (Si−O−Si, Si−O−Al, and Al−O−Al) and tricluster oxygens ($O(Si,Al)_3$) in a variety of silicate, aluminosilicate, and aluminate clusters.[23,33] We have also presented ^{17}O, ^1H, and ^2H NMR results for SiOH in aluminum-free silicate clusters.[23] A drawback of our previous calculation results for the SiOH group is that they were based on clusters optimized with the Hartree−Fock (HF) theory and a moderate basis set (HF/6-31G(d)). The HF method is known to be unsatisfactory in reproducing O−H bond length and hydrogen bonding distance. For accurate representation of the latter, the electron-correlation effect needs to be considered. The density functional theory (DFT) has been found to yield satisfactory O−H bond length, hydrogen-bonding distance, and O−H vibrational frequencies, comparable to those of the more computationally intensive MP2 (Møller−Plesset second-order perturbation theory) method[34] (also see below). In this study, we have optimized the cluster geometries with the DFT method and with a large basis set (6-311+G(2df,p)). We have also investigated how the calculation method (HF vs DFT) and basis set used for the geometry optimization affect the calculated NMR parameters. Furthermore, we have also examined water species that are possibly present not only in aluminum-free silicate systems but also in aluminosilicate systems (SiOH, AlOH, and bridging OH's). With these calculation results, we are in a better position to understand the existing experimental ^1H and ^{17}O NMR data for hydrous silicate glasses and gels. We revisit these data in an attempt to gain further insight into the speciation, the hydrogen-bonding strength, and the dynamics of the dissolved water in these systems.

TABLE 1: Comparison of Calculated Structural Parameters for H_2O and H_2O-H_2O Dimer Molecules at Different Levels of Theory

	H_2O		H_2O-H_2O dimer	
method/basis set	R(O−H) (Å)	∠H−O−H (deg)	R(O−H)[a] (Å)	R(O−H···O) (Å)
HF/3-21G**	0.941	105.8	0.946	2.828
HF/6-31G(d)	0.947	105.5	0.952	2.971
HF/6-31+G(d)	0.947	106.6	0.952	2.963
HF/6-311+G(2df,p)	0.941	106.6	0.946	3.029
B3LYP/6-31+G(d,p)	0.965	105.8	0.973	2.888
B3LYP/6-311+G(2df,p)	0.962	105.3	0.970	2.909
B3LYP/aug-cc-pVTZ[b]	0.962	105.1	0.970	2.917
MP2/6-31+G(d,p)	0.963	105.8	0.973	2.915
MP2/6-311+G(2df,p)	0.961	104.8	0.970	2.907
MP2//aug-cc-pVTZ[b]	0.961	104.1	0.969	2.908
Exp.[b]	0.957[c]	104.5		2.946

[a] Only the R(O−H) for O−H···O linkage is shown, two others are within 0.002 Å of that of the H_2O molecule. [b] See ref 34. [c] Corrected for vibration/rotation. Uncorrected value is 0.972 Å (cf. ref 60).

Calculation Methods

All of the calculations have been performed using the Gaussian 98 program.[35] The approach we have taken is to construct small silicate, aluminosilicate, and aluminate clusters that contain the structural units of interest. In particular, all Si and Al in these clusters are coordinated to four oxygens, resembling those in silicate and aluminosilicate glasses and melts at relatively low pressure. All clusters are terminated at the peripheries by OH. The data analyzed in this study include those on clusters optimized at three different levels of theory: HF/6-31G(d), HF/6-31+G(d), and B3LYP/6-311+G(2df,p), where B3LYP stands for the Becke's three parameter hybrid functional using the correlation functional of Lee, Yang, and Parr,[35] a typical DFT method. The first two are largely a result of earlier calculations.[23,33] Further calculations were carried out on clusters optimized at B3LYP/6-311+G(2df,p), because they yield more reliable O−H and hydrogen-bonding (O−H···O) distances. For example, the O−H and O−H···O distances in H_2O and the H_2O-H_2O dimer are well reproduced (within 0.005 and 0.04 Å of the respective experimental value) at this level of theory (see Table 1 for a comparison).

We have calculated the electric field gradient (EFG) and magnetic shielding tensors using the HF method with the 6-311+G(2df,p) basis set. The quadrupolar coupling constant (C_Q) and EFG asymmetry parameter (η_Q) are calculated using the following equations:

$$C_Q = e^2 q_{zz} Q/h$$

$$\eta_Q = (eq_{xx} - eq_{yy})/eq_{zz}$$

where eQ is the nuclear quadrupole moment of the nucleus of interest and eq_{xx}, eq_{yy}, and eq_{zz} are the components of the EFG tensor at the nucleus in the principal axis system, with $|eq_{zz}| \geq |eq_{yy}| \geq |eq_{xx}|$. Similar to our previous studies,[23,33] we have estimated the nuclear quadrupole moment eQ for ^{17}O and ^2H using the experimentally determined C_Q^O and C_Q^H values for H_2O molecule (10.175 ± 0.067 MHz for ^{17}O and 307.95 ± 0.14 kHz for ^2H)[36] and the ^{17}O and ^2H EFG tensor values for the same molecule calculated at the same level of theory as for the silicate clusters. The advantage of treating the nuclear eQ as an adjustable parameter is that the resultant C_Q is insensitive

TABLE 2: Calculated ^{17}O EFG-Related Parameters for H_2O Ice Ih and Ice II Clusters[a]

	calculated		experimental	
cluster	C_Q^O [b] (MHz)	η_Q^O	C_Q^O (MHz)	η_Q^O
		Ice Ih		
$5H_2O$	7.565	0.983	6.525	0.925
$17H_2O$	7.321	0.994	6.525	0.925
		Ice II, O1[c]		
$5H_2O$	7.784	0.883	6.983	0.865
$17H_2O$	7.436	0.899	6.983	0.865
		Ice II, O2[c]		
$5H_2O$	7.953	0.962	6.983	0.865
$17H_2O$	7.706	0.945	6.983	0.865

	eq_{zz}^O (a.u.)	η_Q^O	C_Q^O (MHz)	η_Q^O
H_2O exp geom, vib. av.	1.8673	0.783	10.175	0.75
H_2O exp geom, equil.	1.8223	0.803	10.175	0.75

[a] Cluster geometries for ice Ih and II are based on crystal structures determined from neutral diffraction at 123 and 110 K, respectively.[38,39] Experimental C_Q^O and η_Q^O data from nuclear quadrupole resonance (NQR) studies at 77 K;[41,42] EFG calculations at HF/6-311+G(2df,p). [b] Normalized to H_2O molecule with experimentally determined, vibrationally averaged geometry. For comparison, the eq_{zz}^O for the H_2O molecule with experimentally determined equilibrium (corrected for vibration) geometry is also given below. The latter was used for normalization in our earlier paper.[37] [c] Experimental NQR data did not resolve these two O sites.[42]

to the basis sets and method used. The calculated C_Q^O for most of the silicate, aluminosilicate, and aluminate clusters has negative values. Because experimental NMR does not normally distinguish the sign of C_Q, unless explicitly noted, the discussions in the rest of the paper refer to the absolute value of C_Q.

The C_Q^O values calculated at the HF/6-311+G(2df,p) level for Si−O−Si, Si−O−Al, and Al−O−Al bridging oxygens in silicate clusters with HF/6-31G(d) or HF/6-31+G(d) geometries have been shown to be in general agreement with experimental NMR data for similar linkages in silicate crystals and glasses.[23,33] Our earlier calculation at the same level of theory on Si−O−Si bridging oxygens in silicate clusters with geometries adopted from the real crystal structures of SiO_2 polymorphs further confirmed the reliability of such a calculation:[37] The relative differences in C_Q^O among different oxygen sites and their η_Q^O values are within uncertainties of the respective experimental NMR data; the absolute C_Q^O values are about 0.2−0.3 MHz lower than the experimental values, when normalized to H_2O with vibrationally uncorrected geometry (note that in our original paper[37] the C_Q^O was normalized to H_2O with equilibrium geometry). Thus, at least for bridging oxygens and non-hydrogen-bonded OH (in H_2O molecule), we are confident about the reliability of the calculated C_Q^O values. To test to what extent we can reproduce C_Q^O for hydrogen-bonded OH, we have also performed test calculations for two H_2O ice polymorphs (II and Ih). In the ice II structure, all of the hydrogen atoms are fully ordered with O−H···O distances between 2.77 and 2.84 Å,[38] whereas in ice Ih the hydrogen atoms are fully disordered, with a O−H···O distance of 2.76 Å.[39,40] We have performed calculations for clusters of $5H_2O$ (two shells of H_2O molecules) and $17H_2O$ (three shells of H_2O molecules), with geometries adopted from the real crystal structure determined by neutron diffraction at low temperature. The differences in the calculated values for the central H_2O between these two cluster sizes are $\leq$0.3 MHz for C_Q^O and $\leq$0.02 for η_Q^O (see Table 2). These differences are rather small, suggesting that the $17H_2O$ cluster size is near convergence in terms of ^{17}O EFG-related parameters. The calculated C_Q^O (Table 2) (normalized to those of H_2O molecule with experimentally determined, vibrationally uncorrected geometry) are 0.4−0.8 MHz higher than the experimental values obtained by nuclear quadrupole resonance at 77 K.[41,42] The agreement is thus poorer than for Si−O−Si bridging oxygens in SiO_2 polymorphs. It should be remembered that the H positions in H_2O ices have not been measured to such high precision as Si and O positions in silica polymorphs, and there are suggestions that the O−H distances determined by neutron diffraction are probably in large error.[42] Thus, the discrepancy in the calculated C_Q^O values from experimental data may at least partly be due to uncertainties with the crystal structure. We may thus conclude that the ab initio MO calculation method yields reliable C_Q^O values (at least to within 1 MHz, possibly better) for bridging oxygens, non-hydrogen-bonded OH, and hydrogen-bonded OH linkages.

For the C_Q^H, both experimental NMR data on various crystalline non-silicate compounds, including H_2O ice and hydrates,[18] and our calculations on silicate and aluminosilicate clusters[23] (also see below) and H_2O clusters (unpublished data) have shown that it is largely a function of O−H distance and hydrogen-bonding distance, regardless of the state of OH's (H_2O or hydroxyls). As is shown below, our calculated values are within about 20−30 kHz (about 10% discrepancy) of the experimental data in the C_Q^H vs O−H···O distance plot.

The ^1H and ^{17}O isotropic chemical shifts (δ_i^H and δ_i^O; in ppm) are calculated relative to the respective reference using the following equation:

$$\delta_i^{H,O}(\text{cluster}) = \sigma_i^{H,O}(\text{reference}) - \sigma_i^{H,O}(\text{cluster})$$

where σ_i is the isotropic magnetic shielding (in ppm) from the MO calculations. The reference clusters are a tetramethylsilane (TMS, $Si(CH_3)_4$) cluster (T_d symmetry) for ^1H and H_2O (C_{2v}) for ^{17}O. We have adopted the continuous set of gauge transformations (CSGT) method for the magnetic shielding tensor calculations, to compare directly with our earlier calculations for silicate clusters.[23]

The calculated δ_i^H, like C_Q^H, turns out to be largely a function of O−H distance and hydrogen-bonding distance[23] (also see below). This is in accord with experimental data on various crystalline non-silicate compounds, including H_2O ice and hydrates.[19] As is shown below, the calculated δ_i^H values agree to about 2 ppm with the experimentally observed trend in the δ_i^H vs O−H···O distance plot.

For δ_i^O, we have shown previously[23,33] that the calculated values for Si−O−Si, Si−O−Al, and Al−O−Al bridging oxygens in various silicate, aluminosilicate and aluminate clusters at the level of theory described here (with the CSGT method) are in broad good agreement with the respective experimental NMR data for similar local structures in crystalline and amorphous silicates or aluminosilicates. However, a detailed test with different basis set and theory (HF, B3LYP, and MP2) suggests that the absolute δ_i^O values vary considerably depending on the method and theory used, although the relative differences in δ_i^O among bridging oxygens, tricluster oxygens, and SiOH groups do not vary as much.[33] The relative difference in δ_i^O for Si−O−Si sites in SiO_2 polymorphs have been reproduced to about 10 ppm, with the gauge-independent atomic orbital (GIAO) method at HF/6-311+G(2df,p).[37] Thus, the calculated value for δ_i^O should be viewed with a larger uncertainty (at least >10 ppm in terms of relative difference) than for C_Q^O or δ_i^H. Nevertheless, the trend for different types of OH groups might be useful.

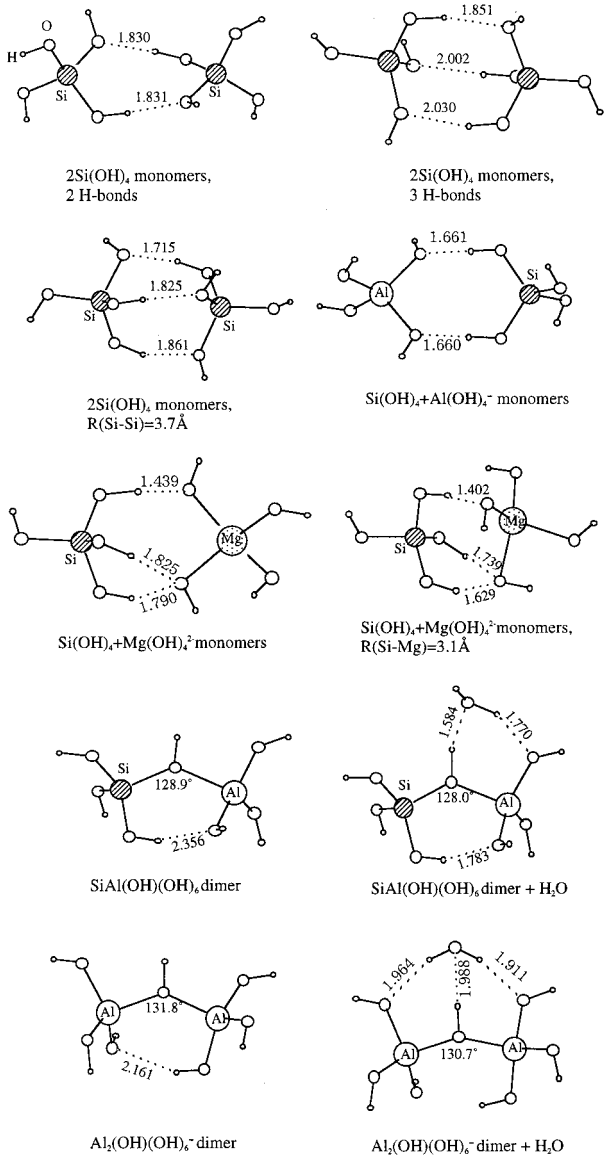

Figure 1. Representative clusters optimized at B3LYP/6-311+G(2df,p). Dotted lines represent hydrogen bonding. Numbers are hydrogen-bonding H···O distances in Å.

Results and Discussion

1. Geometries. The geometries for most of the clusters optimized at HF/6-31G(d) and HF/6-31+G(d) have already been reported in two previous papers.[23,33] Representative clusters optimized at B3LYP/6-311+G(2df,p) are shown in Figures 1 and 2, and their O−H bond length, H···O and O−H···O distances, and O−H···O angles are tabulated in Table 3. The trends of change in the O−H, H···O, and O−H···O distances with basis set and method (HF vs B3LYP) used for geometry optimization are similar to those seen in the H_2O and H_2O−H_2O dimer clusters (Table 1). Only the B3LYP/6-311+G(2df,p) geometries will be described in this section, although the O−H, H···O and O−H···O distances for the HF/6-31+G(d) geometries can also be found in Table 4. At B3LYP/6-311+G(2df,p), the O−H distances for hydroxyls that do not act as a hydrogen-donor (i.e., are not involved in the O−H···O type hydrogen bonding) are 0.960−0.968 Å for SiOH, 0.957−0.967 Å for AlOH, 0.967 Å for Si(OH)Al, and 0.962 Å for Al(OH)Al.

To obtain cluster geometries with strong hydrogen bonding, we have constructed various freely interacting clusters, including two or three $Si(OH)_4$ monomers, $Si(OH)_4$−$Al(OH)_4^-$ and

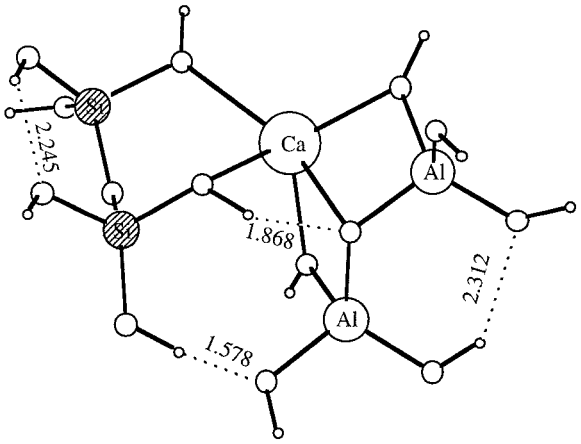

$Ca(Si_2O(OH)_6)(Al_2O(OH)_6)$ double-dimer

Figure 2. Ca-sandwiched $Si_2O(OH)_6$ and $Al_2O(OH)_6^{-2}$ double-dimer cluster optimized at B3LYP/6-311+G(2df,p). Symbols and labels are the same as those in Figure 1.

$Si(OH)_4$−$Mg(OH)_4^{2-}$ two monomers, monomer−H_2O, SiAl(OH)$(OH)_6$ dimer−H_2O, and $Al_2(OH)(OH)_6^-$ dimer−H_2O clusters (Figure 1). For the two $Si(OH)_4$ monomer cluster, both two-hydrogen-bonding and three-hydrogen-bonding configurations are stable (Figure 1). The latter gives somewhat lower energy. We have also performed partial optimization with a fixed Si−Si (or Si−Mg) distance for the $2Si(OH)_4$ and $Si(OH)_4$−$Mg(OH)_4^{2-}$ two-monomer clusters in an attempt to find the geometries that give the shortest hydrogen-bonding distances (Si−Si distance around 3.7 Å for the former and Si−Mg distance around 3.1 Å for the latter). For the $2Si(OH)_4$ cluster, when the Si−Si distance is reduced further beyond this geometry, the hydrogen-bonding distance initially increases, but then the two SiO_4 tetrahedra turn into two edge-sharing SiO_5 pentahedra. For the $Si(OH)_4$−$Mg(OH)_4^{2-}$ cluster, a $(OH)_3Mg$-$OSi(OH)_3^{2-}$ dimer + H_2O configuration is formed at shorter Si−Mg distance. Some of the aluminosilicate clusters we have studied also contain Ca (e.g., Ca− sandwiched $Si_2O(OH)_6$ and $Al_2O(OH)_6^{2-}$ double dimer, see Figure 2). This gives us information about how the coordination of oxygens in SiOH and AlOH to an additional metal cation affects their NMR parameters.

For SiOH, AlOH, and bridging OH's that behave as a hydrogen-donor, the O−H bonds are normally lengthened. There is a general correlation between the O−H bond length, the H···O distance, and the O−H···O distance, with a more rapid rate of O−H bond lengthening at very strong hydrogen bonding (see Tables 3 and 4 and Figure 3). The correlation between the O−H···O angle and either of the O−H, H···O or O−H···O distance is weak, although very strong hydrogen bonding tends to yield large O−H···O angles (Figure 3). This is consistent with earlier observation at HF/3-21G**.[30] It is worth mentioning, however, that although the O−H···O distances for intra-tetrahedral oxygens are sometimes short (e.g., 2.62 Å for the O···O pairs in $Si(OH)_4$ monomer) they are, in general, not associated with long O−H bond length or short H···O distance (e.g., 0.960 and 2.738 Å, respectively, for $Si(OH)_4$ monomer; see Figure 3). In addition, their O−H···O angles (72.9° in Si-$(OH)_4$ monomer) are distinctly smaller than those of intertetrahedral pairs (134.3−178.5°; see Figure 3). These short O−H···O distances are thus not a result of hydrogen bonding but merely reflect the geometry of the SiO_4 tetrahedron. The NMR characteristics of such OH groups are different from those of comparable O−H···O distances with intertetrahedral hydro-

TABLE 3. Calculated ^{17}O and ^{1}H (^{2}H) NMR Parameters for Various OH Groups in Silicate Clusters Optimized at B3LYP/6-311+G(2df,p)[a]

linkage	R(O−H) (Å)	R(H···O) (Å)	R(O−H···O) (Å)	∠O−H···O (deg)	δ_i^O (ppm)	$-C_Q^O$ (MHz)	η_Q^O	δ_i^H (ppm)	C_Q^H (kHz)
				$Si(OH)_4$ Monomer					
Si−O−H	0.9601				12.2	8.1	0.47	2.1	310.2
				$Si(OH)_4-H_2O$					
Si−O−H···O	0.9738	1.903	2.808	153.4	13.4	7.0	0.47	5.5	254.9
Si−O−H	0.9600				12.9	8.1	0.49	2.0	310.4
Si−O−H	0.9604				14.6	8.0	0.46	2.1	309.4
Si−O−H	0.9609				15.6	8.0	0.56	2.1	308.1
				$Si_2O(OH)_6$ Dimer					
Si−O−H	0.9602				10.1	8.1	0.47	2.1	309.7
Si−O−H···O	0.9638	2.547	3.260	130.8	16.9	7.8	0.50	2.8	296.6
Si−O−H	0.9602				14.6	8.0	0.55	2.0	309.7
				$SiAlO(OH)_6^-$ Dimer					
Si−O−H	0.9606				19.0	8.1	0.54	1.1	312.8
Si−O−H···O	0.9842	1.818	2.751	157.0	24.2	6.4	0.58	6.7	225.4
Si−O−H	0.9597				18.3	8.2	0.53	0.8	316.4
Al−O−H	0.9583				−9.9	8.4	0.24	−0.9	328.2
Al−O−H	0.9579				−7.7	8.5	0.26	−0.9	329.5
Al−O−H	0.9582				0.9	8.3	0.31	−0.5	326.7
				$Al_2O(OH)_6^{2-}$ Dimer					
Al−O−H	0.9601				−2.9	8.6	0.28	−1.7	327.7
Al−O−H	0.9608				−2.3	8.4	0.28	−1.3	323.9
Al−O−H	0.9599				−2.8	8.6	0.28	−1.8	328.7
				$Al_3O(OH)_9^{2-}$ Tricluster					
Al−O−H	0.9628				−4.1	8.1	0.30	0.0	309.4
Al−O−H···O	0.9691	2.040	2.943	154.2	−6.6	7.0	0.33	2.5	276.8
Al−O−H	0.9596				3.6	8.6	0.29	−1.1	327.0
				$Si(OH)_4-Al(OH)_4^-$ Two Monomer					
Si−O−H	0.9599				18.3	8.2	0.52	1.0	314.6
Si−O−H	0.9598				17.0	8.2	0.52	0.9	315.4
Si−O−H···O	0.9958	1.661	2.657	177.3	23.3	6.0	0.50	9.3	190.2
Si−O−H···O	0.9958	1.660	2.656	178.5	22.7	6.1	0.50	9.2	190.6
Al−O−H	0.9583				−11.4	8.4	0.23	−0.8	327.8
Al−O−H	0.9579				8.2	8.3	0.37	−0.3	326.5
Al−O−H	0.9583				4.7	8.3	0.35	−0.1	324.8
Al−O−H	0.9577				−5.8	8.5	0.26	−0.9	329.7
				$2Si(OH)_4$ Monomer, 2 H-Bonds					
Si−O−H	0.9603				12.4	8.0	0.47	2.1	309.5
Si−O−H	0.9617				19.3	7.9	0.58	2.4	305.2
Si−O−H	0.9601				12.8	8.1	0.48	2.0	310.2
Si−O−H···O	0.9748	1.830	2.801	174.3	13.8	6.9	0.46	6.0	249.0
				$2Si(OH)_4$ Monomer, 3 H-Bonds					
Si−O−H	0.9604				9.3	8.0	0.48	2.3	308.6
Si−O−H	0.9620				20.2	8.0	0.56	2.3	305.0
Si−O−H	0.9617				19.2	7.9	0.53	2.3	305.4
Si−O−H···O	0.9766	1.851	2.814	168.0	16.7	6.9	0.53	6.3	244.6
Si−O−H	0.9597				5.7	8.1	0.51	2.0	311.2
Si−O−H···O	0.9685	2.030	2.959	160.1	22.1	7.3	0.57	4.1	274.6
Si−O−H	0.9620				22.7	8.0	0.58	2.2	305.6
Si−O−H···O	0.9680	2.002	2.950	165.9	16.4	7.5	0.55	4.4	273.2
				$2Si(OH)_4$ Monomer, 3 H-Bonds (R(Si−Si) = 3.7 Å)					
Si−O−H	0.9642				13.8	8.1	0.52	2.3	301.1
Si−O−H	0.9660				26.7	8.0	0.59	2.7	296.2
Si−O−H	0.9654				24.3	7.9	0.56	2.6	297.1
Si−O−H···O	0.9852	1.715	2.670	162.1	23.2	6.5	0.60	8.0	220.3
Si−O−H	0.9636				10.5	8.1	0.54	2.1	303.4
Si−O−H···O	0.9736	1.861	2.774	154.9	27.8	6.9	0.62	5.5	257.9
Si−O−H	0.9658				26.6	8.0	0.60	2.6	296.7
Si−O−H···O	0.9736	1.825	2.760	159.8	21.7	7.1	0.60	5.9	254.1
				$Si(OH)_4$-$Mg(OH)_4^{2-}$ Two Monomer					
Si−O−H···O	0.9924	1.8252	2.738	151.5	26.7	6.3	0.78	7.3	208.6
Si−O−H	0.9606				13.9	8.2	0.55	0.3	315.7
Si−O−H···O	1.0712	1.439	2.508	175.4	45.5	4.5	0.83	16.0	66.3
Si−O−H···O	0.9954	1.790	2.717	153.3	28.7	6.1	0.79	7.7	200.4
				$Si(OH)_4$-$Mg(OH)_4^{2-}$ Two Monomer (R(Si−Mg) = 3.1 Å)					
Si−O−H···O	1.0040	1.629	2.546	149.6	36.1	5.5	0.83	10.1	173.6
Si−O−H	0.9604				21.0	8.2	0.54	0.0	316.6
Si−O−H···O	1.0693	1.402	2.453	165.9	60.5	4.1	0.89	16.9	65.3
Si−O−H···O	0.9893	1.739	2.600	143.3	35.8	6.1	0.74	8.0	210.0

TABLE 3 (Continued)

linkage	R(O−H) (Å)	R(H···O) (Å)	R(O−H···O) (Å)	∠O−H···O (deg)	δ_i^O (ppm)	$-C_Q^O$ (MHz)	η_Q^O	δ_i^H (ppm)	C_Q^H (kHz)
				$SiAl(OH)(OH)_6$ Dimer					
Si−(OH)-Al	0.9670				27.8	7.2	0.95	4.4	283.6
Si−O−H	0.9600				10.2	8.0	0.48	2.4	308.5
Si−O−H···O	0.9900	1.741	2.673	155.5	23.5	6.4	0.45	8.7	208.1
Si−O−H	0.9610				13.1	7.9	0.45	2.5	306.2
Al−O−H	0.9566				−15.2	8.0	0.23	0.6	324.3
Al−O−H	0.9566				−13.9	8.1	0.19	0.5	325.0
Al−O−H	0.9585				−2.3	8.0	0.34	1.0	318.9
				$SiAl(OH)(OH)_6$ Dimer-H_2O					
Si−(OH)-Al	1.016	1.584	2.564	160.6	33.7	−5.9	0.72	12.5	148.8
Si−O−H	0.9601				10.4	8.0	0.49	2.3	309.1
Si−O−H···O	0.9849	1.783	2.698	153.0	23.9	6.5	0.46	7.8	221.4
Si−O−H	0.9607				13.2	8.0	0.46	2.4	307.5
Al−O−H	0.9593				−3.7	7.9	0.35	0.9	317.2
Al−O−H	0.9565				−13.0	8.1	0.18	0.5	325.2
Al−O−H	0.9575				−3.4	8.1	0.34	0.9	321.6
				$Al_2(OH)(OH)_6^-$ Dimer					
Al−(OH)-Al	0.9624				10.7	7.5	0.67	2.2	303.5
Al−O−H	0.9582				−9.7	8.3	0.24	−0.6	327.4
Al−O−H	0.9572				−12.5	8.4	0.26	−0.6	329.3
Al−O−H	0.9579				−10.6	8.4	0.25	−0.7	328.2
Al−O−H	0.9578				−13.7	8.3	0.26	−0.4	327.3
Al−O−H···O	0.9652	2.161	3.041	150.9	−8.6	7.4	0.23	1.9	290.2
Al−O−H	0.9583				−2.4	8.4	0.28	−0.4	326.0
				$Al_2(OH)(OH)_6^-$ Dimer-H_2O					
Al−(OH)-Al	0.9778	1.988	2.837	143.9	13.7	6.5	0.79	4.9	248.7
Al−O−H	0.9581				−9.6	8.3	0.23	−0.6	327.3
Al−O−H	0.9581				−4.2	8.3	0.28	−0.2	325.7
Al−O−H	0.9585				−1.8	8.3	0.31	−0.3	325.0
Al−O−H	0.9574				−11.3	8.4	0.26	−0.4	328.4
Al−O−H···O	0.9664	2.078	2.965	151.9	−7.8	7.2	0.25	2.3	285.3
Al−O−H	0.9583				−2.7	8.4	0.28	−0.2	325.2
				$Ca(Si_2O(OH)_6)(Al_2O(OH)_6)$ Double Dimer					
Si(Ca)-O−H	0.9629				21.5	7.7	0.69	2.7	299.9
Si(Ca)-O−H···O	0.9860	1.868	2.652	134.3	43.7	6.5	0.55	8.1	222.4
Si−O−H···O	0.9673	2.245	3.033	138.0	15.8	7.5	0.46	4.0	281.8
Si−O−H···O	1.0141	1.578	2.586	171.7	26.9	5.7	0.48	11.9	152.1
Si−O−H	0.9605				11.8	8.0	0.47	2.5	307.1
Si−O−H	0.9606				12.6	7.9	0.58	2.3	307.2
Al(Ca)-O−H	0.9586				23.5	7.7	0.36	1.3	317.9
Al(Ca)-O−H	0.9587				21.1	7.8	0.38	1.1	318.5
Al−O−H···O	0.9645	2.313	3.105	138.9	−11.5	7.4	0.23	1.8	296.6
Al−O−H	0.9565				−11.3	8.2	0.22	−0.1	327.6
Al−O−H	0.9596				4.0	7.9	0.43	1.0	316.0
Al−O−H	0.9568				−6.9	8.2	0.25	0.0	326.7

[a] NMR parameters calculated at HF/6-311+G(2df,p) (CSGT method for shielding tensor) on geometries optimized at B3LYP/6-311+G(2df,p) for all clusters including H_2O and TMS. Chemical shift relative to H_2O (σ_i^O, H_2O = 310.4 ppm) for ^{17}O and relative to TMS (σ_i^H, TMS = 31.8 ppm) for ^1H: δ_i^O (ppm) = 310.4 − σ_i^O; δ_i^H (ppm) = 31.8 − σ_i^H. Quadrupolar coupling constant normalized to those of H_2O (C_Q^O, H_2O = 10.175 MHz and C_Q^H, H_2O = 307.95 kHz), using the calculated eq^O_{zz} (1.8313 au) and eq^H_{zz} (0.48490 au) for H_2O: C_Q^O (MHz) = $eq^O_{zz}/1.8313 \times 10.175$ and C_Q^H (kHz) = $eq^H_{zz}/0.484\,90 \times 307.95$.

gen bonding but belong to OH groups with no (or very weak) hydrogen bonding (e.g., large C_Q^O and small δ_i^H; see Table 3). Contrary to earlier postulations,[20,43] such intratetrahedral "hydrogen bonding" cannot yield significantly reduced OH stretching frequencies or large δ_i^H that are characteristic of strong hydrogen bonding. All of the subsequent discussions of hydrogen bonding (O−H···O) refer to intertetrahedral pairs.

A convenient way to describe the strength of hydrogen bonding is to divide the range of O−H···O distances into three regions: A distance of >2.7 Å is generally described as weak hydrogen bonding, a distance in the range of 2.5−2.7 Å is described as strong hydrogen bonding, and a distance <2.5 Å is described as very strong hydrogen bonding.[44] The O−H···O distances described here (2.45−3.26 Å) encompass all three regions and also cover the whole range displayed by silanols in silicate minerals (O−H···O distances down to 2.46 Å[45]). We have found that SiOH in the Si−O−H system only forms relatively weak hydrogen bonding (O−H···O distances ≥2.67 Å), even if two $Si(OH)_4$ monomers are arbitrarily brought close to one another (see Figure 1). SiOH can form stronger hydrogen bonding with an oxygen from an AlOH linkage (O−H···O distances down to 2.59 Å) and even stronger hydrogen bonding with an oxygen from a MgOH linkage (O−H···O distances down to 2.45 Å; see Figure 1). The fact that very strong hydrogen bonding has been identified for SiOH only in crystalline silicates that contain network-modifying cations (e.g., Mg, Ca, and Na)[45] is consistent with this observation. The AlOH group has a tendency to behave as a hydrogen acceptor and only forms Al−O−H···O type hydrogen bonding among themselves in aluminate clusters. Even so, the hydrogen bonding is usually weak (O−H···O distance ≥2.94 Å; see Figures 1 and 2). This can be understood from the small charge of Al^{3+}, compared to that of Si^{4+}. Bridging OH's, especially Si(OH)Al, on the other hand, have a tendency to form relatively strong

TABLE 4. Calculated ^{17}O and ^{1}H (^{2}H) NMR Parameters for Various OH Groups in Silicate Clusters Optimized at HF/6-31+G(d)[a]

linkage	R(O−H) (Å)	R(H···O) (Å)	R(O−H···O) (Å)	δ_i^O (ppm)	$-C_Q^O$ (MHz)	δ_i^H (ppm)	C_Q^H (kHz)
			$Al(OH)_4^-$ Monomer				
Al−O−H	0.9456			−2.7	8.5	−1.4	324.9
			$Si_2O(OH)_6$ Dimer				
Si−O−H	0.9469			14.3	8.2	1.8	307.2
Si−O−H···O	0.9497	2.648	3.320	21.1	8.0	2.4	297.6
Si−O−H	0.9469			18.5	8.1	1.7	307.5
			$SiAlO(OH)_6^-$ Dimer				
Si−O−H	0.947			22.9	8.3	0.9	310.0
Si−O−H···O	0.9601	1.943	2.831	25.3	6.9	4.9	254.8
Si−O−H	0.946			21.2	8.4	0.6	314.1
Al−O−H	0.9455			−5.3	8.4	−1.2	323.8
Al−O−H	0.9452			−3.1	8.5	−1.2	324.8
Al−O−H	0.9452			2.2	8.4	−0.9	323.5
			$Al_2O(OH)_6^{2-}$ Dimer				
Al−O−H	0.9467			0.7	8.6	−1.9	323.9
Al−O−H	0.9472			1.5	8.5	−1.6	321.0
Al−O−H	0.9465			−0.1	8.6	−2.0	324.9
			$Al_3O(OH)_9^{2-}$ Tricluster				
Al−O−H	0.9483			−0.2	8.2	−0.4	310.9
Al−O−H···O	0.9517	2.065	2.937	−2.5	7.1	1.8	286.0
Al−O−H	0.9462			6.1	8.6	−1.4	323.5
			$AlSi_2O(OH)_9$ Tricluster				
Al−O−H	0.946			−0.5	8.0	0.8	313.8
Al−O−H	0.9444			−5.0	8.1	0.5	317.7
Al−O−H	0.9462			4.2	8.1	0.6	314.3
Si−O−H···O	0.9555	2.032	2.813	24.9	7.2	4.6	271.7
Si−O−H···O	0.9596	1.859	2.723	21.0	7.0	6.2	251.6
Si−O−H···O	0.956	2.076	2.919	24.6	7.6	4.8	267.7
Si−O−H···O	0.9491	2.548	3.075	22.2	8.1	2.8	297.8
Si−O−H···O	0.949	2.566	2.909	23.0	7.9	2.5	298.4
Si−O−H	0.9479			19.9	8.2	2.1	304.0
			$Si(OH)_4$-$Al(OH)_4^-$ Two Monomer				
Si−O−H	0.9464			21.2	8.3	0.9	311.7
Si−O−H	0.9463			19.7	8.3	0.8	312.3
Si−O−H···O	0.9678	1.770	2.736	24.5	6.5	7.1	225.7
Si−O−H···O	0.9681	1.770	2.738	24.1	6.5	7.2	225.3
Al−O−H	0.9456			−6.8	8.5	−1.1	323.2
Al−O−H	0.9449			8.4	8.4	−0.8	323.4
Al−O−H	0.9452			5.1	8.4	−0.6	322.3
Al−O−H	0.9451			−0.2	8.5	−1.3	325.4
			$Ca(SiAlO(OH)_6)_2$ Double Dimer				
Si(Ca)-O−H	0.948			28.5	7.8	2.3	302.6
Si−O−H···O	0.9605	1.948	2.804	24.2	6.9	5.4	254.6
Si−O−H	0.9472			17.0	8.1	1.9	306.3
Si(Ca)-O−H	0.9483			28.9	7.8	2.5	301.1
Si−O−H···O	0.9602	1.946	2.806	24.0	7.0	5.3	255.2
Si−O−H	0.947			17.6	8.1	1.9	306.7
Al(Ca)-O−H	0.9464			15.2	7.8	1.1	311.8
Al−O−H	0.9434			−7.5	8.3	−0.1	322.8
Al−O−H	0.9448			1.5	8.1	0.1	318.9
Al(Ca)-O−H	0.9463			14.2	7.8	0.9	312.7
Al−O−H	0.9434			−7.7	8.2	−0.1	322.6
Al−O−H	0.9447			1.3	8.1	0.1	319.1
			$Ca(Al_2O(OH)_6)_2$ Double Dimer				
Al(Ca)-O−H	0.9436			11.2	8.2	−0.4	324.8
Al−O−H	0.9465			−2.2	8.4	−1.1	321.4
Al−O−H	0.9462			−4.2	8.5	−1.3	323.1
			$Ca(Si_2O(OH)_6)(Al_2O(OH)_6)$ Double Dimer				
Si(Ca)-O−H	0.9508			26.5	7.7	2.4	295.4
Si(Ca)-O−H···O	0.9581	2.250	2.837	39.6	7.2	5.1	267.5
Si−O−H···O	0.9524	2.347	3.095	19.6	7.8	3.4	285.9
Si−O−H···O	0.9778	1.718	2.677	26.7	6.2	9.0	202.2
Si−O−H	0.9477			16.1	8.1	2.3	303.5
Si−O−H	0.948			17.2	8.0	2.1	303.3
Al(Ca)-O−H	0.946			24.1	7.8	0.8	314.6
Al(Ca)-O−H	0.9462			22.1	7.8	0.6	314.5
Al−O−H···O	0.9495	2.534	3.272	−7.8	7.7	1.0	302.4
Al−O−H	0.9443			−5.8	8.3	−0.4	322.7

TABLE 4 (Continued)

linkage	R(O−H) (Å)	R(H···O) (Å)	R(O−H···O) (Å)	δ_i^O (ppm)	$-C_Q^O$ (MHz)	δ_i^H (ppm)	C_Q^H (kHz)
			$Ca(Si_2O(OH)_6)(Al_2O(OH)_6)$ Double Dimer				
Al−O−H	0.9472			4.4	8.0	0.4	312.7
Al−O−H	0.9441			−2.4	8.3	−0.5	323.1

[a] NMR parameters calculated at HF/6-311+G(2df,p) (CSGT method for shielding tensor) on geometries optimized at HF/6-31+G(d) for all clusters including H_2O and TMS. Chemical shift relative to H_2O (σ_i^O, H_2O = 318.9 ppm) for ^{17}O and relative to TMS (σ_i^H, TMS= 32.0 ppm) for ^1H: δ_i^O (ppm) = 318.9 − σ_i^O and δ_i^H (ppm) = 32.0 − σ_i^H. Quadrupolar coupling constant normalized to those of H_2O (C_Q^O, H_2O = 10.175 MHz and C_Q^H, H_2O = 307.95 kHz), using the calculated eq^O_{zz} (1.7783 au) and eq^H_{zz} (0.53515 au) for H_2O: C_Q^O (MHz) = eq^O_{zz}/1.7783 × 10.175; C_Q^H (kHz) = eq^H_{zz}/0.535 15 × 307.95.

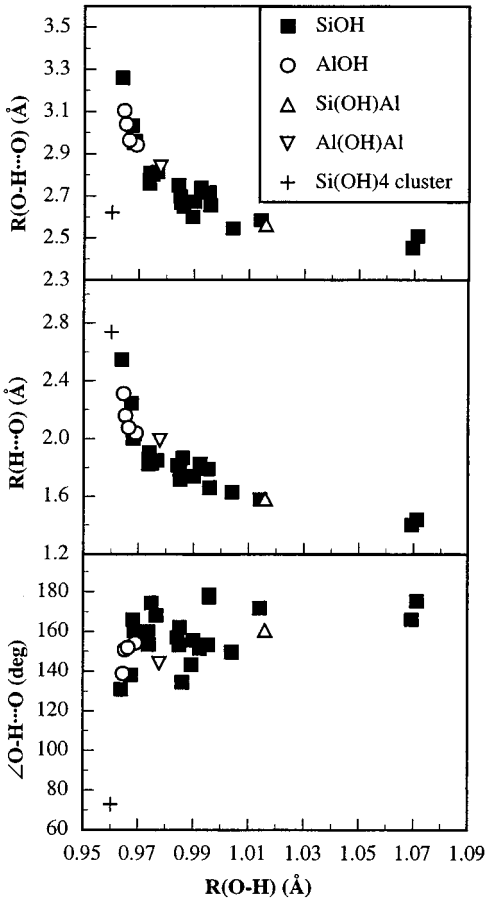

Figure 3. O-H···O distance (top), H···O distance (middle), and O−H···O angle (bottom) plotted as a function of O−H bond length for SiOH, AlOH, and bridging OH's with inter-tetrahedral H-bonding in clusters optimized at B3LYP/6-311+G(2df,p). Also plotted for comparison are data for SiOH with apparent intratetrahedral "H-bonding" in the $Si(OH)_4$ cluster (see text for discussion).

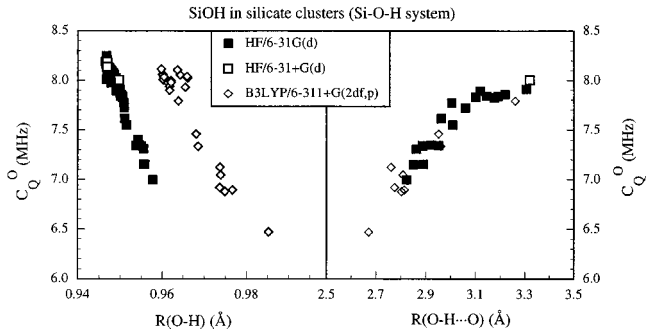

Figure 4. Calculated ^{17}O quadrupolar coupling constant (C_Q^O) as a function of O−H bond length (left) and O−H···O distance (right) for SiOH linkages from silicate clusters in the Si−O−H system optimized at different levels of theory. All EFG tensors calculated at HF/6-311+G-(2df,p).

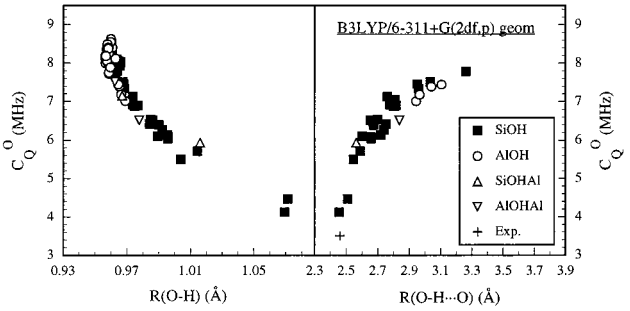

Figure 5. Calculated ^{17}O quadrupolar coupling constant (C_Q^O) as a function of O−H bond length (left) and O−H···O distance (right) for SiOH, AlOH, and bridging OH's in clusters optimized at B3LYP/6-311+G(2df,p). All EFG tensors calculated at HF/6-311+G(2df,p). Ca-coordinated SiOH and AlOH (Si(Ca)OH and Al(Ca)OH) are not distinguished from those without Ca coordination in this figure. Also plotted are experimental data for Si(K)OH in crystalline $KHSi_2O_5$ phase.[25]

hydrogen bonding with other oxygens (O−H···O distance of 2.56 Å for the Si(OH)Al linkage, see Figure 1). This feature is in accord with the acidic nature of such sites (also referred to as Brønsted acidic sites) in zeolites.

2. ^{17}O NMR Characteristics. Plotted in Figure 4 are the calculated C_Q^O vs O−H bond length and C_Q^O vs O−H···O distance for SiOH linkages in the Si−O−H system optimized at HF/6-31G(d), HF/6-31+G(d) and B3LYP/6-311+G(2df,p). Optimization at B3LYP/6-311+G(2df,p) in general yields shorter hydrogen-bonding distances and longer O−H bonds for the same cluster, compared with that at HF/6-31G(d) or HF/6-31+G(d). Nevertheless, remarkably, the calculated C_Q^O values for clusters optimized at all three levels fall on the same trend in the C_Q^O vs O−H···O distance plot, though displaced in the C_Q^O vs O−H bond length plot (Figure 4). Thus, the C_Q^O results on clusters optimized with the HF method are still reliable in terms of their relationship with the hydrogen-bonding strength (O−H···O distance). It is also worth mentioning that SiOH linkages that are hydrogen-bonded to an oxygen from either another SiOH group or a H_2O, fall on the same trend in the C_Q^O vs O−H bond length and C_Q^O vs O−H···O distance plots.

In clusters that contain aluminum or a network-modifying cation (Mg), SiOH can form even stronger hydrogen bonding with an oxygen from an AlOH or MgOH linkage, and thus, the overall C_Q^O range extends to lower values (to 4.1 Å for a Si−O−H···OH linkage with a O−H···O distance of 2.45 Å; see Figure 5). The C_Q^O value decreases faster with decreasing O−H···O distance near the very strong hydrogen-bonding region (O−H···O distance <2.5 Å; see Figure 5). This behavior has also been observed for O−H stretching vibration frequency of OH groups (cf. ref 30). The calculated C_Q^O for SiOH with very strong hydrogen bonding agree reasonably well (within 0.6 MHz) with the recently reported experimental value (3.5 MHz[25]) for a SiOH site in crystalline $KHSi_2O_5$ that has an O−H···O

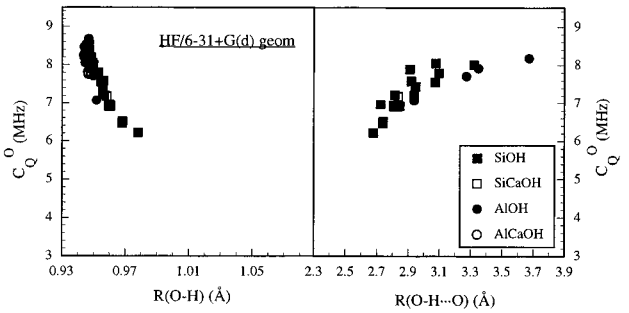

Figure 6. Calculated ^{17}O quadrupolar coupling constant (C_Q^O) as a function of O−H bond length (left) and O−H···O distance (right) for SiOH and AlOH in clusters optimized at HF/6-31+G(d). All EFG tensors calculated at HF/6-311+G(2df,p).

distance of 2.46 Å[46] (see Figure 5). The large range of C_Q^O values for SiOH, from around 8 MHz for non-hydrogen-bonded linkages to 4.1 MHz for those with very strong hydrogen bonding, signify the importance of hydrogen bonding.

Non-hydrogen-bonded AlOH has C_Q^O values about 7.9−8.6 MHz, overlapping with those of non-hydrogen-bonded SiOH (Tables 3 and 4, Figures 5 and 6). Because AlOH tends to behave as a hydrogen acceptor (Al(OH)···H) when forming hydrogen bonding with a SiOH, their C_Q^O are in general not reduced. Only when Al forms hydrogen bonding among themselves (in aluminate clusters) do some of the AlOH act as a hydrogen donor. In this case, their C_Q^O fall nearly on the same trend (though somewhat lower) as SiOH in the C_Q^O vs O−H bond length and C_Q^O vs O−H···O distance plots (see Figures 5 and 6). The smallest calculated C_Q^O for AlOH is 7.0 MHz for a Al−O−H···O linkage with an O−H···O distance of 2.94 Å (see Table 3, Figure 5). Therefore, AlOH are expected to yield broad peaks in single-pulse ^{17}O MAS or static NMR spectra, unless there are motions that reduce their peak widths.

The C_Q^O of oxygens in SiOH or AlOH that are coordinated with additional Ca cations (Si(Ca)OH, Al(Ca)OH) fall on the same trend as those not coordinated to Ca in the C_Q^O vs O−H bond length and C_Q^O vs O−H···O distance plots (see Figure 6). Thus, the effect of cation interaction on the C_Q^O of SiOH or AlOH is manifested through its effect on the hydrogen-bonding strength.

Bridging OH's (Si(OH)Al, Al(OH)Al) that are not hydrogen-bonded to another oxygen give relatively large C_Q^O (7.2 MHz for Si(OH)Al, 7.5 MHz for Al(OH)Al). The two clusters we have calculated for the hydrogen-bonded situation yield a C_Q^O of 5.9 MHz for a Si(OH)Al with a hydrogen-bonding O−H···O distance of 2.56 Å and 6.5 MHz for a Al(OH)Al with a hydrogen-bonding O−H···O distance of 2.84 Å. The C_Q^O for Si(OH)Al and Al(OH)Al fall on the same trend as SiOH and AlOH in the C_Q^O vs O−H bond length and C_Q^O vs O−H···O distance plots (see Figure 5). Clearly, the number of clusters containing bridging OH's that we have investigated is limited. It has been shown that the hydrogen bonding of a Si(OH)Al site could be very strong (O−H···O distance <2.5 Å) when interacting with two H_2O molecules in a larger cluster.[47] Thus, the range of C_Q^O for Si(OH)Al is expected to extend to <4 MHz, like those of SiOH. It is therefore difficult to distinguish between bridging OH's (at least Si(OH)Al) and SiOH of comparable hydrogen bonding strengths on the basis of the C_Q^O parameter.

The calculated EFG asymmetry parameter η_Q^O for SiOH groups are in the range 0.46−0.89 for clusters optimized at B3LYP/6-311+G(2df,p) (see Table 3). The calculated η_Q^O for AlOH groups are smaller (0.18−0.38, see Table 3). On the other hand, the calculated η_Q^O for bridging OH groups are somewhat larger (0.72−0.95 for Si(OH)Al and 0.67−0.79 for Al(OH)Al; see Table 3). As a result of the large η_Q^O, the C_Q^O of the Si(OH)Al group in the $Si(OH)(OH)_6$ dimer changes sign from negative to positive upon hydrogen bonding with a water molecule (see Table 3).

The calculated δ_i^O for SiOH does not show clear dependence on the hydrogen-bonding strength or any other single structural parameter [23] (also data in Tables 3 and 4). The calculated δ_i^O for SiOH are in the range of 5−61 ppm (Table 3) for clusters optimized at B3LYP/6-311+G(2df,p), overlapping with the range for a smaller number of clusters optimized at HF/6-31G(d) (14−34 ppm[23]) or HF/6-31+G(d) (14−29 ppm, see Table 4). Those for AlOH are lower (−15 to +8 ppm for the B3LYP/6-311+G(2df,p) geometries; Table 3). The AlOH and SiOH groups that are also coordinated to a Ca (Al(Ca)OH and Si(Ca)OH) tend to give somewhat larger δ_i^O than those without Ca coordination (see Tables 3 and 4). This resembles the trend displayed by bridging oxygens (e.g., SiOAl and AlOAl).[33] The calculated δ_i^O for bridging OH's (28−34 ppm for Al(OH)Si and 11−14 ppm for Al(OH)Al) overlap with those of SiOH (see Table 3).

Combining the result for C_Q^O and δ_i^O, we expect that SiOH and bridging OH's of comparable hydrogen-bonding strengths yield similar ^{17}O NMR parameters. Both types of OH sites produce a large range of C_Q^O values depending on the strength of hydrogen bonding. The AlOH group distinguishes itself from the other types of OH's by its tendency not to form strong Al−O−H···O type hydrogen bonding and thus is expected to yield large C_Q^O (on the order of 8 MHz).

3. ^1H and ^2H NMR Parameters. Our earlier study on aluminum-free silicate clusters optimized at HF/6-31G(d) showed good correlation between the calculated δ_i^H and C_Q^H values and the O−H distance and O−H···O distance.[23] Like C_Q^O, the calculated δ_i^H and C_Q^H values for SiOH, AlOH, and bridging OH's in clusters optimized with different basis set and method fall on the same trend in the plot with O−H···O distance, though displaced in the plot with O−H bond length (compare Figures 7 and 8). Thus the calculated δ_i^H and C_Q^H for SiOH from our earlier work are still reliable in terms of their relationship with the hydrogen-bonding distance. The δ_i^H and C_Q^H for AlOH and bridging OH's also fall on the same trend (though with scatter) as SiOH in the plots against O−H and O−H···O distances (see Figures 7 and 8). Furthermore, our calculation result for H_2O clusters of various sizes (up to $6H_2O$) also falls on the same trend in these two plots (not shown). Thus, the δ_i^H and C_Q^H values of OH groups are dominated by the O−H bond length and hydrogen-bonding strength and are insensitive to the types of cations to which they are bonded.

Good correlation between δ_i^H and hydrogen-bonding O−H···O distance has also been reported for experimental NMR data of organic and inorganic nonsilicate compounds (including H_2O ice). Eckert et al.[19] have compiled the available experimental ^1H NMR data for these crystalline compounds (with O−H···O distances mostly in the range 2.4−2.9 Å) and have fitted the experimental data with a linear equation: $\delta_i^H(\text{ppm}) = 79.05 - 25.5R(\text{O}-\text{H}\cdots\text{O})$ (Å) (where R(O−H···O) stands for the O−H···O distance). Our calculated δ_i^H for OH groups with O−H···O distances ≤2.9 Å are within about 2 ppm of the fitted curve (Figures 7 and 8). Considering the scatter of experimental data (about ± 2 ppm, see Figure 12 of ref 19), the agreement is fairly reasonable. At larger O−H···O distances, our calculated

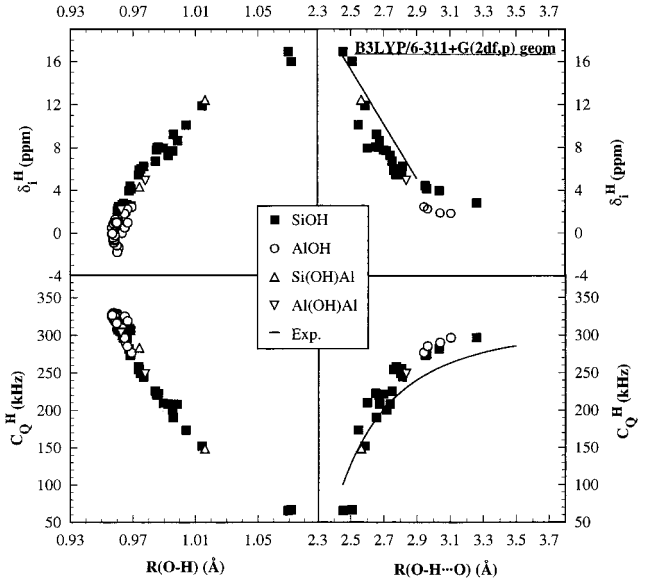

Figure 7. Calculated ^{1}H isotropic chemical shift (δ_i^H; top) and ^{2}H quadrupolar coupling constant (C_Q^H; bottom) as a function of O−H bond length (left) and O−H···O distance (right) for SiOH, AlOH, and bridging OH's in clusters optimized at B3LYP/6-311+G(2df,p). All shielding and EFG tensors calculated at HF/6-311+G(2df,p). Ca-coordinated SiOH and AlOH (Si(Ca)OH and Al(Ca)OH) are not distinguished from those without Ca coordination in this figure. Curves for experimental data of non-silicates are δ_i^H (ppm) = 79.05 − 25.5R(O−H···O) from ref 19 and C_Q^H (kHz) = 311.0 − 223.8/[R(O−H···O) − 1.433]^3 from ref 18. The upper limits of R(O−H···O) for these curves are those of the experimental data.

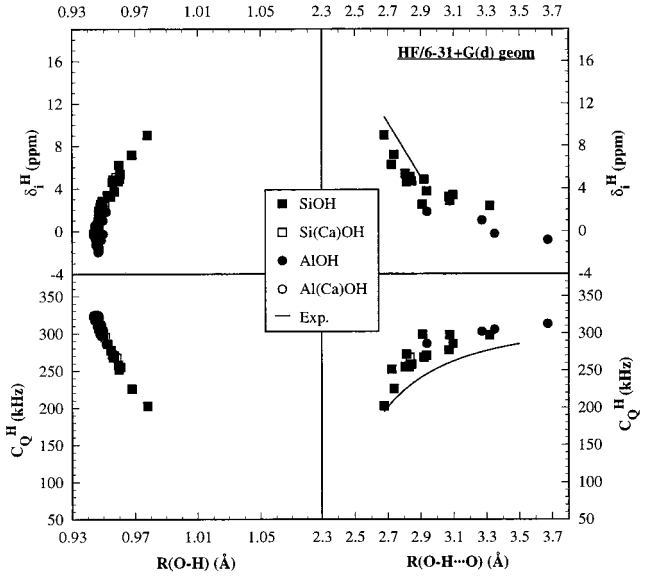

Figure 8. Calculated ^{1}H isotropic chemical shift (δ_i^H; top) and ^{2}H quadrupolar coupling constant (C_Q^H; bottom) as a function of O−H bond length (left) and O−H···O distance (right) for SiOH and AlOH in clusters optimized at HF/6-31+G(d). All shielding and EFG tensors calculated at HF/6-311+G(2df,p). Curves for experimental data are the same as those in Figure 7.

δ_i^H levels off (Figures 7 and 8), whereas there are few experimental data available in this range.

Similar correlation between C_Q^H and R(O−H···O) has also been reported for experimental ^{2}H NMR data of organic and inorganic nonsilicate compounds (see ref 18 and reference therein). Like the experimental δ_i^H, the calculated C_Q^H increases with increasing O−H···O distance and levels off at large O−H···O distances. There is a maximum of about 10% (20−30 kHz) deviation between our calculated values and the experimental values for nonsilicates, with the calculated values leveling off at a shorter O−H···O distance than the experimental data (see Figures 7 and 8). The agreement is, nevertheless, fairly satisfactory.

In brief, both the δ_i^H and the C_Q^H of SiOH, AlOH, and bridging OH's show good correlations with the O−H bond length and the hydrogen-bonding distance. The values of the δ_i^H and C_Q^H parameters are thus more an indicator of the hydrogen-bonding strength and are not themselves unique for distinguishing different types of hydroxyls or molecular H_2O.

It should also be mentioned that the calculated O−H stretching frequency values for hydroxyls in various silicate clusters[30,31] show a pattern very similar to those described here for δ_i^H and C_Q^H. Experimental data of O−H stretching frequency for nonsilicates also exhibit good correlation with the hydrogen-bonding distance [48] and C_Q^H (e.g., ref 49). Thus, the δ_i^H, C_Q^H, and O−H stretching frequency are complementary to one other and all yield information about the strength of hydrogen-bonding. Because these different techniques are sensitive to motions with different frequencies, a comprehensive study using all these techniques may yield information about both the hydrogen-bonding strength and the dynamics of the dissolved water species.

4. Implications to the Speciation and Dynamics of Water in Silica Gel and Hydrous Silicate Glasses. Our calculations and existing theoretical and experimental data together suggest that the C_Q^O of hydroxyls and the δ_i^H, C_Q^H, and O−H stretching frequency of both hydroxyls and molecular H_2O are all dominated by the strength of hydrogen bonding. It is probably difficult to distinguish between SiOH with moderate to very strong hydrogen bonding from bridging OH's on the basis of single pulse ^{1}H and ^{17}O NMR or vibrational spectroscopy, although more sophisticated NMR methods, such as the double resonance technique, may yield such information. AlOH tends to form only weak, if any, Al−O−H···O type hydrogen bonding. Thus, AlOH, together with weakly hydrogen-bonded SiOH, are expected to yield relatively large C_Q^O, C_Q^H, and O−H stretching frequency and small δ_i^H.

Although it is not the intent of this study to predict the NMR characteristics of "free" OH's (e.g., NaOH and MgOH) and molecular H_2O in silicates, there are a number of experimental ^{17}O data published for such groups in crystalline phases. Free OH's in crystalline hydrates and hydrous silicates in general yield relatively large C_Q^O (≥6.5 MHz, see ref 50 for a compilation). Our calculation suggests that the free OH group (e.g., MgOH) tends to behave as a hydrogen acceptor in silicates and aluminosilicates, if participating in hydrogen bonding at all (see Figure 1). Thus, their C_Q^O, like those of AlOH, are in general not likely to be lowered to any large extent by hydrogen bonding. The reported C_Q^O for molecular H_2O in analcime ($NaAlSi_2O_6 \cdot H_2O$; O−H···O distances in the range 3.34−3.67 Å[51]) from experimental ^{17}O MAS NMR is 7.6 ± 0.2 MHz.[24] The C_Q^O for molecular H_2O in various forms of H_2O ices (II, Ih, V, VI, VIII, and IX) determined by nuclear quadrupole resonance at 77 K [41,42,52] are in a small range of 6.5−7.1 MHz. The hydrogen-bonding strengths of H_2O in these ices are weak (e.g., the O−H···O distance is 2.88 Å for ice Ih[40]). Thus, molecular H_2O with weak hydrogen-bonding strengths (O−H···O distances ≥2.8 Å) are probably in the range of 6.5−7.5 MHz. Those with stronger hydrogen bonding are expected to yield smaller C_Q^O.

With this knowledge, we reexamine the existing IR, Raman, and ^{17}O and ^{1}H NMR data for silica gel and hydrous silicate

and aluminosilicate glasses, in an attempt to gain further insight into the speciation of the dissolved water in silicate glasses and their hydrogen-bonding strength and dynamics. From the experimental ^{1}H NMR and vibrational spectra, we first estimate the degree of hydrogen bonding for the dissolved water species. We then use this information to estimate their expected C_Q^O (expected ^{17}O NMR peak width), if the water species were SiOH, AlOH, or bridging OH's. Significant deviation (to smaller values) of the experimental ^{17}O NMR peak widths from the expected C_Q^O may indicate motional narrowing and/or the absence of such OH groups.

4.1. Silica Gels. There have been numerous IR studies on silica gels. For example, the IR spectrum for Carbosil, a pure fumed silica degassed at 27 °C, shows a broad asymmetric peak with maxima near 3520 cm^{-1} and 3660 cm^{-1}, in addition to a narrow peak at 3747 cm^{-1}.[53] These may correspond to hydrogen-bonded SiOH with O−H···O distances of 2.95 and 3.2 Å for the former two, and non-hydrogen-bonded SiOH for the latter, according to the correlation of ref 48. The ^{1}H CRAMPS (combined rotation and multiple-pulse spectroscopy) spectra of silica gels evacuated at room temperature or 200 °C yield a broad asymmetric peak centered at 3.3 ppm and a narrow peak at 1.7 ppm.[17,54] Both peaks have been attributed to SiOH.[17,54] From the correlation between δ_i^H and O−H···O distance[19] (also see Figure 7), the broad 3.3 ppm peak may correspond to weakly hydrogen-bonded SiOH with peak O−H···O distance of about 2.95 Å, and the 1.7 ppm peak may be from non-hydrogen-bonded SiOH. Thus both IR and ^{1}H NMR data suggest that a large population of the SiOH group are weakly hydrogen-bonded with O−H···O distances centered around 2.9−3.0 Å.

We may predict their C_Q^O on the basis of our calculation result (Figure 4). Non-hydrogen-bonded SiOH are expected to have a C_Q^O around 8 MHz, and moderately hydrogen-bonded SiOH populations with a peak O−H···O distance at 2.9 Å are expected to give peak C_Q^O around 7 MHz. The estimated C_Q^O for SiOH from simulation of single pulse ^{17}O NMR or ^{1}H−^{29}Si CP NMR spectra (with short contact time) of silica gels are about 4.0−4.4 MHz (±1 MHz).[55,56] These values are much lower than the peak C_Q^O of around 7 MHz estimated above. There are two possibilities to this apparent paradox. One is that the ^{17}O NMR is perhaps preferentially detecting SiOH with the strongest hydrogen bonding. However, this would be a fairly small population. More likely, the ^{17}O NMR peak width may not reflect the quadrupolar line shape, but there might be significant motional narrowing. A more recent ^{17}O NMR study[50] has detected two SiOH populations for silica gel; one is similar to that described above, and another exhibits a liquidlike behavior (with isotropic motion), with a peak maximum near 0 ppm. The latter component, if not because of molecular water as the authors have argued, would suggest substantial motion of SiOH in silica gel. It is not unlikely that the broader component that yields an apparent C_Q^O around 4 MHz may also have been motionally narrowed. Thus, at least a portion of the SiOH groups in silica gel is likely to be nonrigid. This should be tested by a careful variable-temperature ^{17}O or ^{2}H NMR study.

4.2. Alkaline Silicate Glasses. Perhaps the most complete experimental data set (IR, Raman, ^{1}H, and ^{17}O NMR) for water species in hydrous silicate glasses are those on alkali silicates, particularly the $Na_2Si_4O_9$ composition. The ^{29}Si NMR and IR data indicate the presence of both molecular H_2O and SiOH in the hydrous $Na_2Si_4O_9$ glasses.[6,8] The IR and Raman spectra contain three peaks in the O−H stretching vibration region centered at 3580, 3000, and 2350 cm^{-1} (corresponding to O−H···O distances of 3, 2.7, and 2.55 Å).[8] The relative areas of these three peaks have been shown to be insensitive to the H_2O/OH ratio, suggesting that both OH and H_2O may contribute to these peaks.[8] The ^{1}H MAS and CRAMPS spectra of these glasses contain two peaks centered at 4.5 and 13 ppm.[6,57] These two peaks have been attributed to SiOH with strong hydrogen bonding (13 ppm) and molecular H_2O (4.5 ppm), respectively. However, in light of our calculation result and the vibrational spectra, it is more plausible that both SiOH and molecular H_2O may contribute to each peak, with the 13 ppm NMR peak corresponding to the 2350 cm^{-1} peak in the IR and Raman spectra and the 4.5 ppm NMR peak corresponding to the 3580 and 3000 cm^{-1} peaks of the latter. An often used characteristic to distinguish between molecular H_2O and OH is the line shape of ^{1}H static NMR spectra or the intensity pattern of the spinning sidebands in the ^{1}H MAS NMR spectra. A rigid H_2O molecule typically gives a Pake (doublet) shape, and hydroxyls typically give a sharp line in the static spectra and a small number of spinning sidebands in the MAS spectra. In fact, a ^{1}H two-dimensional CRAMPS-MAS correlation study suggests that the spinning sidebands of the 13 ppm peak are more intense than those typical of hydroxyls, and the spinning sideband pattern of the 4.5 ppm peak is significantly different from that expected from a Pake pattern of rigid H_2O molecules.[57] These sideband intensity patterns can be easily accounted for if each peak contains contributions from both molecular H_2O and SiOH. In brief, both vibrational spectra and ^{1}H NMR data are consistent with the coexistence of two (or three) populations of SiOH and molecular H_2O, one of which is engaged in strong hydrogen bonding and another (or the other two) is weakly to moderately hydrogen-bonded.

From the estimated hydrogen-bonding strengths of SiOH in hydrous $Na_2Si_4O_9$ glasses, we may predict their ^{17}O NMR parameters. The SiOH with estimated O−H···O distances of 3 and 2.7 Å should yield C_Q^O of about 6.5−7.5 MHz, and those with O−H···O distance centered at 2.55 Å should yield C_Q^O of about 5−6 MHz. Molecular H_2O may also yield two populations: The weakly hydrogen-bonded populations may yield C_Q^O similar to analcime and H_2O ices (6.5−7.5 MHz), whereas another population with strong hydrogen bonding might yield smaller C_Q^O. As mentioned in the Introduction, the experimental ^{17}O NMR study of Xu et al.[24] revealed two ^{17}O NMR peaks that are most likely due to dissolved water species: one is similar to the peak for silica gel (with an apparent C_Q^O of about 4 MHz) and another broader peak similar to that of molecular H_2O in analcime (with a C_Q^O of 7.6 MHz). The former has been attributed to SiOH and the latter to molecular H_2O. However, if both molecular H_2O and SiOH are rigid, the broader peak might equally well be attributed to weakly hydrogen-bonded hydroxyls (SiOH and/or NaOH), in addition to molecular H_2O; the narrower peak may be assigned to strongly hydrogen-bonded SiOH and/or molecular H_2O (?). Whether similar motions of SiOH, as suggested for silica gels above, exist for alkali silicate glasses needs further experimental investigation, preferentially by a variable-temperature ^{17}O NMR study.

4.3. Albite Glass. Controversy remains as to the presence of AlOH, SiOH, NaOH, or bridging OH's in hydrous albite glasses.[9−15] The Raman and IR spectra of hydrous albite glasses[58,59] show a main peak centered at 3535 cm^{-1} (with an estimated O−H···O peak distance of 2.95 Å), with a shoulder at 3250 cm^{-1} on the Raman spectrum that could be due to weakly hydrogen-bonded hydroxyls or molecular H_2O (with estimated O−H···O distance of 2.8 Å).[59] The ^{1}H MAS NMR

spectra of hydrous albite glasses contain a broad peak centered at 3.5−3.8 ppm.[12,13,20] The ^{1}H spin-echo MAS NMR spectra with relatively long evolution times for hydrous glasses in the $NaAlO_2-SiO_2$ system[11] also contain a shoulder near 5−6 ppm and a small, but distinct, peak at 1.5 ppm, in addition to the 3.5 ppm main peak; the relative intensities of the 5−6 and 1.5 ppm peaks increase with increasing $NaAlO_2$ content. The original authors[11] have assigned the 5−6 ppm peak to SiOH, the 3.5 ppm peak to SiOH/AlOH, and the 1.5 ppm peak to AlOH. However, as is clear from our calculation result, this assignment is not necessarily unique. What is certain is that the 5−6 and 3.5 ppm peaks correspond to OH groups (e.g., SiOH, AlOH, or Si(OH)Al) with O−H···O distances of about 2.88 and 2.95 Å, respectively. The 1.5 ppm corresponds to non-hydrogen-bonded OH groups, which could be either AlOH or NaOH, because both have a tendency not to behave as a hydrogen donor. Thus, unlike alkali silicate glasses, a large population of the H_2O/OH species in albite glasses are involved in only weak hydrogen bonding.

The expected C_Q^O for hydroxyls (SiOH, AlOH, or Si(OH)-Al) with O−H···O distances of 2.88 and 2.95 Å are about 7.0 and 7.5 MHz, respectively. Non-hydrogen-bonded AlOH are expected to yield large C_Q^O (around 8 MHz). Non-hydrogen-bonded NaOH, if present, may also yield large C_Q^O. The experimental ^{17}O NMR spectra of hydrous albite glass[24] contain two peaks that are possibly from water species: one is similar to the peak for silica gel (with an apparent C_Q^O of about 4 MHz) and another broader peak similar to that of molecular H_2O in analcime (with a C_Q^O of 7.6 MHz). These peaks resemble those shown by hydrous $Na_2Si_4O_9$ glass, despite the fact that these glasses have very different hydrogen-bonding strengths as revealed by vibrational and ^{1}H NMR spectra. These ^{17}O NMR data have been interpreted in a similar way as for the alkali silicate glasses by the original authors.[24] However, the narrower peak can only be accounted for, like silica gel, if they are from nonrigid hydroxyls (e.g., SiOH and Si(OH)Al) and/or molecular H_2O (?). The broader peak could also be due to weakly hydrogen-bonded, rigid hydroxyls (e.g., SiOH, AlOH, Si(OH)-Al, and NaOH), in addition to molecular H_2O. Again, a variable-temperature ^{17}O NMR study could put some constraint to this issue.

Summary

Our calculations and existing experimental data together suggest that the C_Q^O, δ_i^H, C_Q^H, and O−H stretching frequencies of hydroxyls are all sensitive to the O−H bond length and the strength of hydrogen bonding, with stronger hydrogen bonding resulting in smaller C_Q^O, C_Q^H, and O−H stretching frequencies and larger δ_i^H. SiOH and bridging OH's of comparable hydrogen-bonding strengths produce similar ^{17}O and ^{1}H (^{2}H) NMR parameters. AlOH tends to form only weak, if any, Al−O−H···O type hydrogen bonding. Thus, AlOH, together with weakly hydrogen-bonded SiOH, are expected to yield relatively large C_Q^O, C_Q^H, and O−H stretching frequency and small δ_i^H.

With this information, and with the existing experimental vibrational spectra and ^{1}H NMR data, which allow us to estimate the hydrogen-bonding strengths, we were able to predict the C_Q^O values for hydroxyls in silica gel and hydrous silicate glasses of different compositions. We infer that at least some of the hydroxyls in silica gel and hydrous albite glass, if present, must be nonrigid, because the observed peaks are significantly narrower than expected from C_Q^O. The broad ^{17}O NMR peaks observed for hydrous albite and alkali silicate glasses, originally attributed to molecular H_2O, could equally well be attributed to rigid hydroxyls with weak hydrogen bonding. A variable-temperature ^{17}O NMR study would be helpful to test these possibilities.

Acknowledgment. We would like to thank J. D. Kubicki and an anonymous reviewer for helpful comments and J. F. Stebbins and J.V. Oglesby for sending their paper while still in press. The calculations were mostly performed on a HP Exemplar V2250, funded by the Ministry of Education, Science, Sports and Culture of Japan. X.X. would also like to acknowledge the Hayashi Memorial Foundation for Female Natural Scientists for a research grant. The cluster structures are plotted using the PPC MacMolplt software by Brett Bode.

References and Notes

(1) Kohn, S. C. *Mineral. Mag.* **2000**, *64*, 389.
(2) Stolper, E. *Contrib. Mineral. Petrol.* **1982**, *81*, 1.
(3) Stolper, E. *Geochim. Cosmochim.* **1982**, *46*, 2609.
(4) Silver, L.; Stolper, E. M. *J. Petrol.* **1989**, *30*, 667.
(5) Farnan, I.; Kohn, S. C.; Dupree, R. *Geochim. Cosmochim. Acta* **1987**, *51*, 2869.
(6) Kummerlen, J.; Merwin, L. H.; Sebald, A.; Keppler, H. *J. Phys. Chem.* **1992**, *96*, 6405.
(7) Maekawa, H.; Saito, T.; Yokokawa, T. *J. Phys. Chem. B* **1998**, *102*, 7523.
(8) Zotov, N.; Keppler, H. *Am. Mineral.* **1998**, *83*, 823.
(9) Burnham, C. W. *Geochim. Cosmochim. Acta* **1975**, *39*, 1077.
(10) Mysen, B. O.; Virgo, D. *Chem. Geol.* **1986**, *57*, 303.
(11) Zeng, Q.; Nekvasil, H.; Grey, C. P. *J. Phys. Chem. B* **1999**, *103*, 7406.
(12) Kohn, S. C.; Dupree, R.; Smith, M. E. *Geochim. Cosmochim. Acta* **1989**, *53*, 2925.
(13) Kohn, S. C.; Dupree, R.; Mortuza, M. G. *Chem. Geol.* **1992**, *96*, 399.
(14) Schmidt, B. C.; Riemer, T.; Kohn, S. C.; Behrens, H.; Dupree, R. *Geochim. Cosmochim. Acta* **2000**, *64*, 513.
(15) Zeng, Q.; Nekvasil, H.; Grey, C. P. *Geochim. Cosmochim. Acta* **2000**, *64*, 883.
(16) Bartholomew, R. F.; Schreurs, J. W. H. *J. Non-Cryst. Solids* **1980**, *38/39*, 679.
(17) Bronnimann, C.; Zeigler, R. C.; Maciel, G. E. *J. Am. Chem. Soc.* **1988**, *110*, 2023.
(18) Eckert, H.; Yesinowski, J. P.; Stolper, E. M.; Stanton, T. R.; Holloway, J. *J. Non-Cryst. Solids* **1987**, *93*, 93.
(19) Eckert, H.; Yesinowski, J. P.; Silver, L. A.; Stolper, E. M. *J. Phys. Chem.* **1988**, *92*, 2055.
(20) Kohn, S. C.; Dupree, R.; Smith, M. E. *Nature* **1989**, *337*, 539.
(21) Zavel'sky, V. O.; Bezmen, N. I.; Zharikov, V. A. *J. Non-Cryst. Solids* **1998**, *224*, 225.
(22) Riemer, T.; Schmidt, B.; Behrens, H.; Dupree, R. *Solid State Nucl. Magn. Reson.* **2000**, *15*, 201.
(23) Xue, X.; Kanzaki, M. *Phys. Chem. Miner.* **1998**, *26*, 14.
(24) Xu, Z.; Maekawa, H.; Oglesby, J. V.; Stebbins, J. F. *J. Am. Chem. Soc.* **1998**, *120*, 9894.
(25) Oglesby, J. V.; Kroeker, S.; Stebbins, J. F. *Am. Mineral.* **2001**, *86*, 341.
(26) Sykes, D.; Kubicki, J. D.; Farrar, T. C. *J. Phys. Chem. A* **1997**, *101*, 2715.
(27) Tossell, J. A.; Saghi-Szabo, G. *Geochim. Cosmochim. Acta* **1997**, *61*, 1171.
(28) Fleischer, U.; Kutzelnigg, W.; Bleiber, A.; Sauer, J. *J. Am. Chem. Soc.* **1993**, *115*, 7833.
(29) Kotrla, J.; Nachtigallova, D.; Kubelkova, L.; Heeribout, L.; Doremieux-Morin, C.; Fraissard, J. *J. Phys. Chem. B* **1998**, *102*, 2454.
(30) Kubicki, J. D.; Sykes, D.; Rossman, G. R. *Phys. Chem. Miner.* **1993**, *20*, 425.
(31) Kubicki, J. D.; Apitz, S. E. *Am. Mineral.* **1998**, *83*, 1054.
(32) Kubicki, J. D.; Sykes, D.; Apitz, S. E. *J. Phys. Chem. A* **1999**, *103*, 903.
(33) Xue, X.; Kanzaki, M. *J. Phys. Chem. B* **1999**, *103*, 10816.
(34) Kim, K.; Jordan, K. D. *J. Phys. Chem.* **1994**, *98*, 10089.
(35) Frisch, M. J.; Trucks, G. W.; Schlegel, H. B.; Scuseria, G. E.; Robb, M. A.; Cheeseman, J. R.; Zakrzewski, V. G.; Montgomery, J. A.; Stratmann, R. E.; Burant, J. C.; Dapprich, S.; Millam, J. M.; Daniels, A. D.; Kudin, K. N.; Strain, M. C.; Farkas, O.; Tomasi, J.; Barone, V.; Cossi, M.; Cammi, R.; Mennucci, B.; Pomelli, C.; Adamo, C.; Clifford, S.; Ochterski, J.; Petersson, G. A.; Ayala, P. Y.; Cui, Q.; Morokuma, K.; Malick, D. K.; Rabuck, A. D.; Raghavachari, K.; Foresman, J. B.; Cioslowski, J.; Ortiz, J. V.; Stefanov, B. B.; Liu, G.; Liashenko, A.; Piskorz, P.; Komaromi, I.;

Gomperts, R.; Martin, R. L.; Fox, D. J.; Keith, T.; Al-Laham, M. A.; Peng, C. Y.; Nanayakkara, A.; Gonzalez, C.; Challacombe, M.; Gill, P. M. W.; Johnson, B.; Chen, W.; Wong, M. W.; Andres, J. L.; Gonzalez, C.; Head-Gordon, M.; Replogle, E. S.; Pople, J. A. *Gaussian 98*, revision A.3; Gaussian, Inc.: Pittsburgh, PA, 1998.

(36) Verhoeven, J.; Dymanus, A.; Bluyssen, H. *J. Chem. Phys.* **1969**, *15*, 3330.

(37) Xue, X.; Kanzaki, M. *Solid State Nucl. Magn. Reson.* **2000**, *16*, 245.

(38) Kamb, B.; Hamilton, W. C.; LaPlaca, S. J.; Prakash, A. *J. Chem. Phys.* **1971**, *55*, 1934.

(39) Peterson, S. W.; Levy, H. A. *Acta Crystallogr.* **1957**, *10*, 70.

(40) Kuhs, W. F.; Lehmann, M. S. *J. Phys. Chem.* **1983**, *87*, 4312.

(41) Edmonds, D. T.; Zussman, A. *Phys. Lett.* **1972**, *41A*, 167.

(42) Edmonds, D. T.; Goren, S. D.; Mackay, A. L.; White, A. A. L. *J. Magn. Reson.* **1976**, *23*, 505.

(43) McMillan, P. F.; Remmele, R. L., Jr. *Am. Mineral.* **1986**, *71*, 772.

(44) Emsley, J. *Chem. Soc. Rev.* **1981**, *9*, 91.

(45) Nyfeler, D.; Armbruster, T. *Am. Mineral.* **1998**, *83*, 119.

(46) Malinovskii, Y. A.; Belov, N. V. *Dokl. Akad. Nauk SSSR* **1979**, *246*, 99.

(47) Krossner, M.; Sauer, J. *J. Phys. Chem.* **1996**, *100*, 6199.

(48) Nakamoto, K.; Margoshes, M.; Rundle, R. E. *J. Am. Chem. Soc.* **1955**, *77*, 6480.

(49) Berglund, B.; Vaughan, R. W. *J. Chem. Phys.* **1980**, *73*, 2037.

(50) van Eck, E. R. H.; Smith, M. E.; Kohn, S. C. *Solid State Nucl. Magn. Reson.* **1999**, *15*, 181.

(51) Mazzi, F.; Galli, E. *Am. Mineral.* **1978**, *63*, 448.

(52) Edmonds, D. T.; Goren, S. D.; White, A. A. L. *J. Magn. Reson.* **1977**, *27*, 35.

(53) McDonald, R. S. *J. Phys. Chem.* **1958**, *62*, 1168.

(54) Chuang, I.-S.; Kinney, D. R.; Maciel, G. E. *J. Am. Chem. Soc.* **1993**, *115*, 8695.

(55) Walter, T. H.; Turner, G. L.; Oldfield, E. *J. Magn. Reson.* **1988**, *76*, 106.

(56) Cong, X.; Kirkpatrick, R. J. *Cem. Concr. Res.* **1993**, *23*, 1065.

(57) Schaller, T.; Sebald, A. *Solid State Nucl. Magn. Reson.* **1995**, *5*, 89.

(58) Mysen, B. O.; Virgo, D.; Harrison, W. J.; Scarfe, C. M. *Am. Mineral.* **1980**, *65*, 900.

(59) McMillan, P. F.; Jakobsson, S.; Holloway, J. R.; Silver, L. A. *Geochim. Cosmochim. Acta* **1983**, *47*, 1937.

(60) Cummins, P. L.; Bacskay, G. B.; Hush, N. S. *J. Phys. Chem.* **1985**, *82*, 2002.